Journal of Physics D: Applied Physics

PAPER

BAIN for III-nitride UV light-emitting diodes: undoped electron blocking layer

To cite this article: Wen Gu *et al* 2021 *J. Phys. D: Appl. Phys.* **54** 175104

IOP Publishing Journal of Physics D: Applied Physics
J. Phys. D: Appl. Phys. **54** (2021) 175104 (9pp) https://doi.org/10.1088/1361-6463/abdefc

BAlN for III-nitride UV light-emitting diodes: undoped electron blocking layer

Wen Gu[1,2,3], Yi Lu[2], Rongyu Lin[2], Wenzhe Guo[2], Zihui Zhang[4], Jae-Hyun Ryou[5], Jianchang Yan[1], Junxi Wang[1], Jinmin Li[1] and Xiaohang Li[2]

[1] Research and Development Center for Solid State Lighting, Institute of Semiconductors, Chinese Academy of Sciences, Beijing 100083, People's Republic of China
[2] Advanced Semiconductor Laboratory, King Abdullah University of Science and Technology, Thuwal 23955-6900, Saudi Arabia
[3] Center of Materials Science and Optoelectronics Engineering, University of Chinese Academy of Sciences, Beijing 100049, People's Republic of China
[4] Institute of Micro-Nano Photoelectron and Electromagnetic Technology Innovation, School of Electronics and Information Engineering, Hebei University of Technology, Key Laboratory of Electronic Materials and Devices of Tianjin, 5340 Xiping Road, Beichen District, Tianjin 300401, People's Republic of China
[5] Department of Mechanical Engineering, Advanced Manufacturing Institute (AMI), and Texas Center for Superconductivity at UH (TcSUH), University of Houston, Houston, TX 77204-4006, United States of America

E-mail: yanjc@semi.ac.cn and xiaohang.li@kaust.edu.sa

Received 10 October 2020, revised 29 December 2020
Accepted for publication 22 January 2021
Published 12 February 2021

Abstract

The undoped BAlN electron-blocking layer (EBL) is investigated to replace the conventional AlGaN EBL in light-emitting diodes (LEDs). Numerical studies of the impact of variously doped EBLs on the output characteristics of LEDs demonstrate that the LED performance shows heavy dependence on the p-doping level in the case of the AlGaN EBL, while it shows less dependence on the p-doping level for the BAlN EBL. As a result, we propose an undoped BAlN EBL for LEDs to avoid the p-doping issues, which a major technical challenge in the AlGaN EBL. Without doping, the proposed BAlN EBL structure still possesses a superior capacity in blocking electrons and improving hole injection compared with the AlGaN EBL having high doping. Compared with the $Al_{0.3}Ga_{0.7}N$ EBL with a doping concentration of 1×10^{20} cm^{-3}, the undoped BAlN EBL LED still shows lower droop (only 5%), compatible internal quantum efficiency (2% enhancement), and optical output power (6% enhancement). This study provides a feasible route to addressing electron leakage and insufficient hole injection issues when designing ultraviolet LED structures.

Keywords: LED, BAlN, undoped, EBL

(Some figures may appear in colour only in the online journal)

1. Introduction

AlGaN-based (III-N) ultraviolet (UV) light-emitting diodes (LEDs) have aroused widespread interests over the past few decades due to their various potential applications in purification, bio-detection, medical treatment, next-generation data storage, and lithography [1]. As a substitute for the conventional mercury lamp, UV LEDs are potentially energy efficient, long lifetime, compact, and environmentally friendly. However, the low efficiency and output optical power of the UV LEDs have hampered their adoption in various applications [2]. The currently developed LEDs operating in UV spectral regions still suffer from relatively low external quantum efficiency and substantial efficiency droop effect [3, 4]. The main reasons for the low efficiency have been identified to be the insufficient hole injection into the

active region [5] and severe electron leakage out of the active region [6]. The commonly used electron-blocking layer (EBL) possesses several concerning issues. The electronic band edge profiles can be bent because of the polarization-induced electrostatic field, which may increase the hole injection barrier and further deteriorate the output performance of the LEDs [7]. Moreover, sufficient p-doping level AlGaN EBL is preferable for blocking electrons [8]. However, the activation energy of widely used p-dopants, e.g. Mg, dramatically rises with increasing Al mole fraction in the AlGaN layer, which makes the ionization of acceptors more challenging [9]. Furthermore, the diffusion of Mg atoms from the p-region to the active region is more severe in high-Al composition structures [10]. The induced Mg-related defects in multiple quantum wells (MQWs) will form nonradiative recombination centers, which are detrimental to the improvement of internal quantum efficiency (IQE) [11]. Besides, the Mg-induced defect will scatter electrons, leading to a low electron mobility [12].

To address the issues associated with the electron leakage, the hole injection, and the p-EBL, various solutions in the layer structures have been proposed. A superlattice was used as the EBL to suppress electron leakage and improve the overall performance of UV LEDs [13]. A quaternary AlInGaN EBL was also employed to reduce the polarization charge density in the heterostructure interface, which facilitates the reduction in band bending of the EBL [14]. Moreover, an EBL-free UV LED structure was proposed by utilizing graded-composition AlGaN quantum barriers (QBs) to realize better electron blocking and hole injection as opposed to the conventional structure with a p-EBL [15]. Researchers also designed the hole injection layers inserted between EBL and MQWs to effectively relieve the polarization-induced valence band bending [16]. Moreover, EBLs with graded composition [17], V-shaped structures [18], two-step tapered structures [19, 20] as well as polarization doped layers [21] show favorable potentials for UV LEDs. However, most of these methods could still suffer from the Mg diffusion issue.

Boron-containing III-N alloys, especially BAlN, are emerging wide-bandgap materials for optoelectronic and power devices. Recently, researchers have successfully grown BAlN/AlN and BAlN/AlGaN superlattices [22, 23]. The epitaxial growth of monocrystalline wurtzite BAlN structures with boron content as high as 11% and 14.4% have been demonstrated [24]. Liu *et al* have calculated the spontaneous polarization (SP) and piezoelectric (PZ) constants of BAlN using hexagonal reference structures [25]. The results also revealed that the heterointerface polarization can be modulated by adjusting the boron composition, which is beneficial for designing polarization-related electronic devices. Importantly for UV LEDs, the band alignment of BAlN/(Al)GaN heterostructure is extremely advantageous for electron confinement and hole injection. The valence and conduction band edges of $B_{0.14}Al_{0.86}N$ are reportedly 0.2 eV lower and 2.1 eV higher, respectively, than those of GaN [26, 27]. Thus, the BAlN EBL is promising to supersede the conventional AlGaN EBL because of the possibility of suppressing electron leakage effectively without severely deteriorating hole injection.

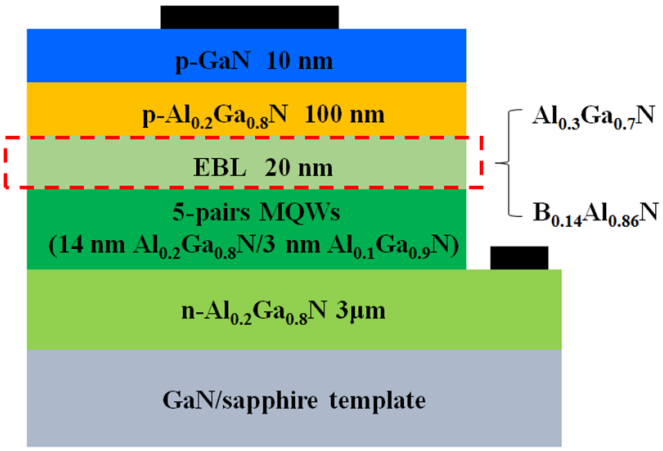

Figure 1. A schematic cross-sectional structure of UV LEDs with variously doped $Al_{0.3}Ga_{0.7}N$ or $B_{0.14}Al_{0.86}N$ EBLs.

In this study, motivated by the conduction and valence band offset properties, $B_{0.14}Al_{0.86}N$ is employed as an alternative to $Al_{0.3}Ga_{0.7}N$ for the EBL in UV LEDs. First, we systematically investigate the effect of p-doping in the $Al_{0.3}Ga_{0.7}N$ EBLs with various doping levels on the output performance of LEDs. The result shows that the p-doping level of an EBL has a great influence on the effective barrier heights of the conduction and valence bands. The high p-doping level in the $Al_{0.3}Ga_{0.7}N$ EBL decreases the valence band offset and increases the conduction band offset, facilitating hole injection and the confinement of electrons, respectively. Meanwhile, we further investigate the $B_{0.14}Al_{0.86}N$ EBL, which shows the same tendency on effective band barrier heights as the $Al_{0.3}Ga_{0.7}N$ EBL. However, the conduction and valence bands of $B_{0.14}Al_{0.86}N$ EBL can maintain relatively high and low offsets, respectively, even with decreasing the Mg doping concentration. Finally, we propose an innovative undoped $B_{0.14}Al_{0.86}N$ EBL for UV LED with superior performance to avert the challenging p-doping issue in high-Al composition layers.

2. Structures and parameters

Figure 1 presents a schematic cross-sectional structure of AlGaN LEDs including either the conventional $Al_{0.3}Ga_{0.7}N$ EBL or the proposed $B_{0.14}Al_{0.86}N$ EBL. The software we used for simulation is the Advanced Physical Models of Semiconductor Devices (APSYS) program [28]. The conventional structures are grown on a GaN/sapphire template, followed by a 3 μm-thick n-$Al_{0.2}Ga_{0.8}N$ layer doped with silicon at a concentration of 5×10^{18} cm^{-3} (n-$Al_{0.2}Ga_{0.8}N$:Si, 3 μm, (Si) = 5×10^{18} cm^{-3}). The active region is composed of five $Al_{0.1}Ga_{0.9}N$ (3 nm each) quantum wells (QWs) (emitting at 344 nm) and six $Al_{0.2}Ga_{0.8}N$ (14 nm each) QBs. Above the last QB is a 20 nm-thick p-$Al_{0.3}Ga_{0.7}N$ EBL with various doping levels ($Al_{0.3}Ga_{0.7}N$:Mg, 20 nm, (Mg) = 0, 1×10^{15}, 1×10^{16}, 1×10^{17}, 1×10^{18}, 1×10^{19}, 1×10^{20} cm^{-3}). Then, a p-$Al_{0.2}Ga_{0.8}N$:Mg layer (100 nm, (Mg) = 2×10^{19} cm^{-3}) and a p-GaN layer (10 nm, (Mg) = 1×10^{20} cm^{-3}) are deposited

Table 1. Material parameters used in the simulation.

Material parameters	GaN	AlN	$B_{0.14}Al_{0.86}N$
Lattice constant a (Å)	3.189	3.112	3.027
Lattice constant c (Å)	5.185	4.981	4.798
Bandgap (eV)	3.4	6.1	5.7
Crystal-field splitting (eV)	0.010	−0.169	−0.169
Spin–orbital splitting (eV)	0.017	0.019	0.019
Electron effective mass (c-axis)	0.2	0.32	0.32
Electron effective mass (transverse)	0.2	0.30	0.29
A1	−7.21	−3.86	2.72
A2	−0.44	−0.25	0.77
A3	6.68	3.58	0.40
A4	−3.46	−1.32	0.77
A5	−3.40	−1.47	1.57
A6	−4.90	−1.64	0.29
Affinity (eV)	3.3	1.4	1.2
Mg activation energy (meV)	170	500	170
Elastic constant C_{33} (GPa)	398	373	480
Elastic constant C_{13} (GPa)	106	108	107
PZ constant e_{31} (C m^{-2})	−0.3582	−0.6691	−0.6935
PZ constant e_{33} (C m^{-2})	0.6149	1.6422	1.7037
Spontaneous polarization (C m^{-2})	1.3389	1.3334	1.3834
Piezoelectric polarization on GaN/sapphire template (C m^{-2})	0	−0.1229	−0.2630
Total polarization on GaN/sapphire template (C m^{-2})	1.3389	1.2105	1.1204

in sequence. For the proposed structures, a $B_{0.14}Al_{0.86}N$ EBL with the same thickness and changes in p-doping levels as the $Al_{0.3}Ga_{0.7}N$ EBL is used. The other layers remain the same as the conventional structures. Both LED structures are designed to be 300 × 300 μm^2 in size.

We assume the conduction/valence band offset ratio of $Al_{0.2}Ga_{0.8}N/Al_{0.1}Ga_{0.9}N$ MQWs is 0.7/0.3 [29]. The SP and PZ constants of $B_{0.14}Al_{0.86}N$ and $Al_xGa_{1-x}N$ ($x = 0$, 0.1, 0.2, 0.3) are from [25, 30], which have proven to be accurate in calculating the polarization of III-N materials [31]. The lattice constant and elastic constants of BAlN alloy we adopted are from [25]. Besides, the affinity of $B_{0.14}Al_{0.86}N$ is 0.9 eV, which has been demonstrated by Sun *et al* [26]. The bandgap of $B_{0.14}Al_{0.86}N$ is set as 5.7 eV. Other parameters of BAlN for calculating band profiles could be found in [32]. The energy bandgap of $Al_xGa_{1-x}N$ alloys is estimated using equation (1), where b is a bowing constant and is chosen to be 0.94 [33], x is the Al content

$$E_g(Al_xGa_{1-x}N)=xE_g(AlN)+(1-x)E_g(GaN)-bx(1-x). \quad (1)$$

The Auger recombination coefficient and Shockley–Read–Hall recombination lifetime are chosen as 1.0×10^{-30} cm^{-3} [34] and 50 ns, respectively. The radiative recombination rate is set to be 2×10^{-11} cm^3 s^{-1} [35]. The screening factor is set to 40%, which is a commonly used value for calculating the polarization-induced built-in interface charges [36]. The operating temperature and background loss are estimated to be 300 K [37] and 2000 m^{-1} [38], respectively. Although the p-$B_{0.14}Al_{0.86}N$ has not been demonstrated in the experiment yet, the acceptor activation energy of $B_{0.14}Al_{0.86}N$ should be similar to that of GaN because of their analogous valence band edge [26]. The effective mass of $B_{0.14}Al_{0.86}N$ is from [32]. The activation energy of GaN or $B_{0.14}Al_{0.86}N$ is supposed to be 170 meV [39], and the activation energy of $Al_xGa_{1-x}N$ is assumed to be 270 meV [40]. Generally accepted material parameters, including effective mass, electron and hole mobility values are applied to $Al_xGa_{1-x}N$ and GaN layers [41]. Other parameters can be found in table 1.

3. Effects of p-doping level in EBLs

The p-doping level of EBL is a critical factor that deserves a considerable attention in designing high-performance LED structures. To evaluate the effects of EBLs at different doping levels on the performance of LEDs, we design the EBLs with a series of Mg doping concentrations (as described in part 2). Figure 2 shows the electronic band edge profiles for the LED structures with an $Al_{0.3}Ga_{0.7}N$ EBL and a $B_{0.14}Al_{0.86}N$ EBL with Mg doping concentrations from 1×10^{18}, 1×10^{19} to 1×10^{20} cm^{-3} at an injection current of 90 mA. The E_{Fn} and E_{Fp} are the quasi-Fermi energy levels of electrons and holes, respectively. As the Mg doping concentration in the EBL increases, the effective barrier height of the conduction band (defined as $\Phi_e = E_c - E_{Fn}$) can increase from 195 to 261 meV for $Al_{0.3}Ga_{0.7}N$ EBL structures in figure 2(a). While for $B_{0.14}Al_{0.86}N$ EBL structures, Φ_e can increase from 1.212 to 1.541 eV shown in figure 2(b). The significantly large Φ_e is because the lager conduction band offset between the $Al_{0.2}Ga_{0.4}N$ QB and $B_{0.14}Al_{0.86}N$ EBL. For both structures, the enhanced Φ_e suppresses the electron overflow out of the active region, indicating better capacities of confining electrons and reducing current leakage. As for the valence band, the effective barrier height (defined as $\Phi_h = E_{Fp} - E_v$) decreases with

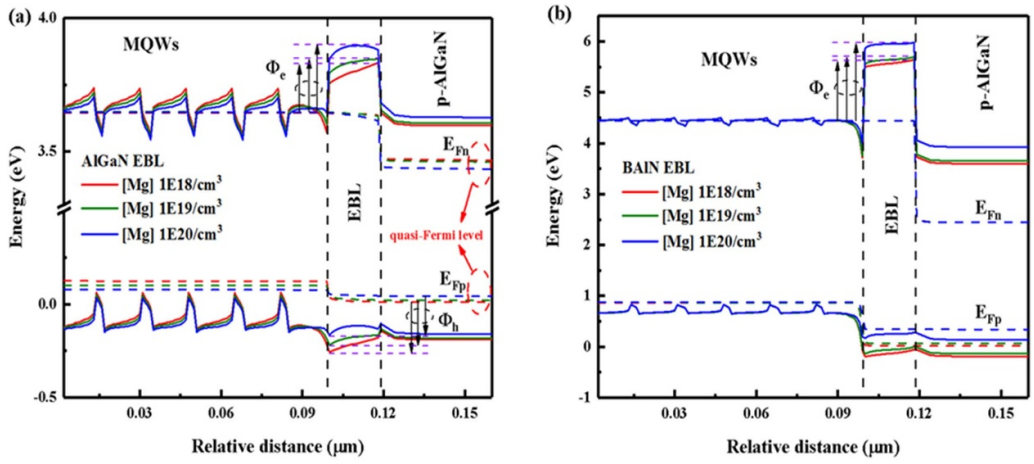

Figure 2. Electronic band edge profiles at an injection current of 90 mA for the LED structures with (a) $Al_{0.3}Ga_{0.7}N$ EBL and (b) $B_{0.14}Al_{0.86}N$ EBL at various Mg doping concentrations.

Table 2. Barrier height of $Al_{0.3}Ga_{0.7}N$ and $B_{0.14}Al_{0.86}N$ EBL structures with various doping concentrations at 90 mA.

Doping concentration of EBL	$Al_{0.3}Ga_{0.7}N$ EBL structures		$B_{0.14}Al_{0.86}N$ EBL structures	
	Φ_e (eV)	Φ_h (eV)	Φ_e (eV)	Φ_h (eV)
1×10^{18} cm^{-3}	0.195	0.274	1.212	0.214
1×10^{19} cm^{-3}	0.211	0.246	1.265	0.210
1×10^{20} cm^{-3}	0.261	0.215	1.541	0.178

increasing Mg doping concentration, suggesting an enhanced hole injection capability for both structures. The modification of the barrier heights in the EBL region can be explained by the fact that the quasi-Fermi energy level of holes will become closer to the valence band edge as the Mg doping concentration increases. The detailed information of Φ_e and Φ_h under different Mg doping concentrations are shown in table 2. It is noted that the large Φ_e and diminutive Φ_h of $B_{0.14}Al_{0.86}N$ EBL are more favorable for the blocking of electrons and enhancing hole injection.

To verify the analysis shown in figure 2, we further study the electron and hole concentrations for both LED structures, as shown in figure 3. The electron leakage in both structures decreases with increasing Mg doping concentrations, as shown in figure 3(a). This phenomenon stems from the enlarged Φ_e as the increase of Mg doping concentration, which suppresses the electrons in the active region overflowing to the p-region. Comparing both LED structures, the LEDs with a $B_{0.14}Al_{0.86}N$ EBL show more significantly reduced electron leakage, even when the doping concentration reduces to a lower level such as 1×10^{18} cm^{-3} due to the relatively high Φ_e. The electron and hole concentrations in the active region increase with the increase of p-doping levels for the LEDs with an $Al_{0.3}Ga_{0.7}N$ EBL, resulting from the enlarged Φ_e and reduced Φ_h, respectively (shown in figures 3(b) and (c)). Because of the large and small barrier heights of the conduction and valence bands, the carrier concentrations in QWs show less difference for the LEDs with a $B_{0.14}Al_{0.86}N$ EBL. Based on the aforementioned results, a higher p-doping level in the $Al_{0.3}Ga_{0.7}N$ or $B_{0.14}Al_{0.86}N$ EBL is preferable for the enhancement of hole injection and blocking electrons. However, the $B_{0.14}Al_{0.86}N$ EBL structures with low p-doping level can still possess high performance while the performance of $Al_{0.3}Ga_{0.7}N$ EBL structures with low p-doping level is seriously deteriorated.

Figure 4 shows the effect of the EBL with various doping levels on the IQE for both LED structures. The LEDs with an $Al_{0.3}Ga_{0.7}N$ EBL exhibit an overall improvement in efficiency with increasing Mg doping concentration in the EBL. The increased IQE can be attributed to the enhanced hole injection and reduced electron leakage. Moreover, the efficiency droop ratio is reduced to 8% with the highest p-doping level for the LEDs with an $Al_{0.3}Ga_{0.7}N$ EBL. The value of efficiency droop ratio is calculated using equation (2), where the IQE_{max} is the peak efficiency value and the IQE_{90} is the value of efficiency at 90 mA. For the LEDs with a $B_{0.14}Al_{0.86}N$ EBL, the IQE shows a slight increase with higher Mg doping concentration, ascribed to the superior electron blocking capability and nearly consistent hole injection capability for all $B_{0.14}Al_{0.86}N$ EBLs with different doping levels. The efficiency droop ratio of the LEDs with a $B_{0.14}Al_{0.86}N$ EBL can still sustain at 5%, even when the doping concentration reduces to 1×10^{18} cm^{-3}, at which doping level the efficiency droop is significant for the LED with an $Al_{0.3}Ga_{0.7}N$ EBL. All of the peak efficiency value for the LEDs with $B_{0.14}Al_{0.86}N$ EBLs can reach as high as 74%, higher than that for any one of the LEDs with an $Al_{0.3}Ga_{0.7}N$ EBL. Apparently, the efficiency of the LEDs with $B_{0.14}Al_{0.86}N$ EBLs is less sensitive to the doping concentration, while high Mg doping is imperative for AlGaN EBL to acquire the high-efficiency UV LED

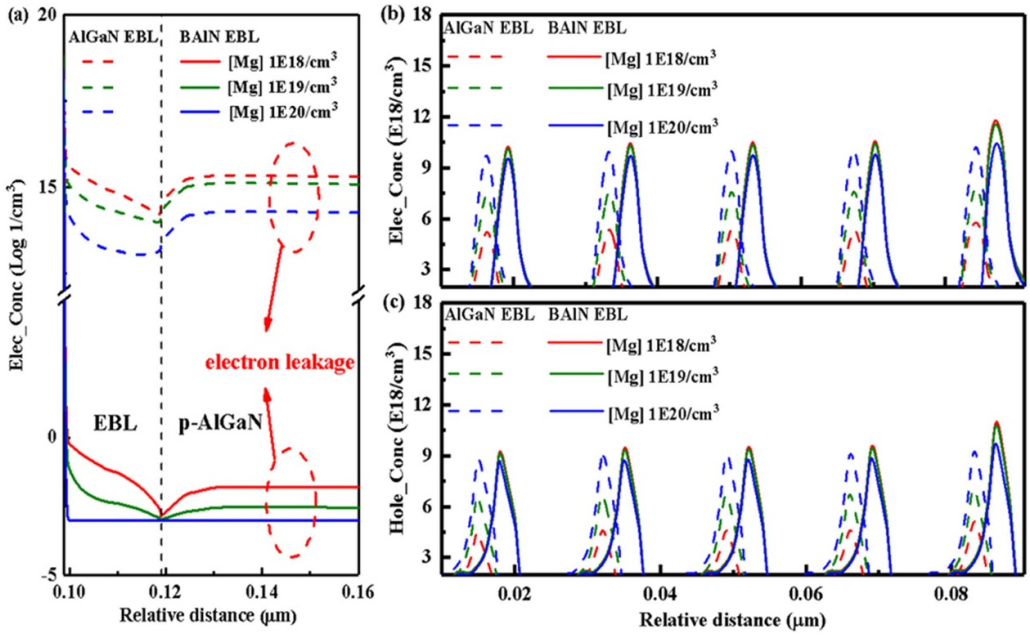

Figure 3. (a) Electron leakage in the p-$Al_{0.2}Ga_{0.8}N$ layer, (b) electron concentration, and (c) hole concentration in QWs at an injection current of 90 mA for the LED structures with $Al_{0.3}Ga_{0.7}N$ and $B_{0.14}Al_{0.86}N$ EBLs at various Mg doping levels. For better observation, we shift electron and hole concentration of $B_{0.14}Al_{0.86}N$ EBL structures in (b) and (c) to the right by 3 nm.

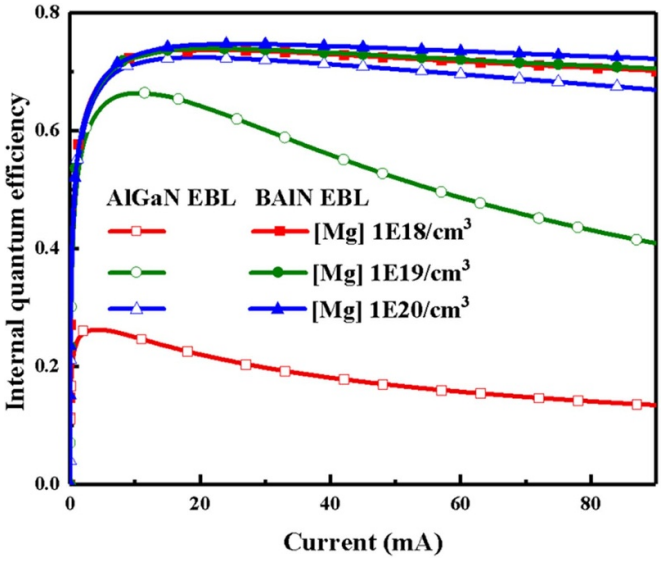

Figure 4. Effect of p-doping level on IQE for $Al_{0.3}Ga_{0.7}N$ and $B_{0.14}Al_{0.86}N$ EBL LED structures at various Mg doping levels.

$$\text{Efficiency droop ratio} = \frac{\text{IQE}_{\max} - \text{IQE}_{90}}{\text{IQE}_{\max}} \times 100\%. \qquad (2)$$

Figure 5 shows the comparisons of current–voltage (*I*–*V*) characterization curves and output powers for both LED structures. The threshold voltage and resistance of these LED structures are presented in table 3. The threshold voltage and resistance decrease with increasing Mg doping for both LED structures, resulting from the increased carrier concentration. However, the degree of change is different. The threshold voltage and resistance of the LEDs with a $B_{0.14}Al_{0.86}N$ EBL decrease substantially, whereas those of the LEDs with an $Al_{0.3}Ga_{0.7}N$ EBL decrease slightly. The higher threshold voltage and resistance of the LEDs with a $B_{0.14}Al_{0.86}N$ EBL are due to that the flow of charge carrier is hindered by the higher barrier height. The LED with an $Al_{0.3}Ga_{0.7}N$ EBL having the highest p-doping level shows a remarkable improvement of output power when compared with that having the lowest doping level as shown in figure 5(b). Even with ten times higher Mg doping concentration than the lowest-doping-level $Al_{0.3}Ga_{0.7}N$ EBL, the output power of $Al_{0.3}Ga_{0.7}N$ EBL LEDs can still increase by 208%. As for the output power of the LEDs with a $B_{0.14}Al_{0.86}N$ EBL having the highest p-doping level, a maximum value of 235 mW can be achieved. Nearly the same output powers for the LEDs with a $B_{0.14}Al_{0.86}N$ EBL are attributed to the perfect electron blocking capability and slightly increased hole injection. As expected, the LEDs with a $B_{0.14}Al_{0.86}N$ EBL having relatively low doping still show enlarged output power compared to the LEDs with an $Al_{0.3}Ga_{0.7}N$ EBL having the highest doping level. It further confirms that the low-doping-level $B_{0.14}Al_{0.86}N$ EBL is still vitally significant in designing high-performance UV LEDs. The wall-plug efficiency (WPE) of both LED structures is defined as the ratio of the total optical output power to the input electrical power. Although the LED with a $B_{0.14}Al_{0.86}N$ EBL having the highest doping level shows a slight reduction in WPE as compared with the LEDs with an equally doped $Al_{0.3}Ga_{0.7}N$ EBL, the LEDs with a $B_{0.14}Al_{0.86}N$ having the lowest doping can still maintain the WPE at 51.2%.

We conclude that the performance of the LEDs with an $Al_{0.3}Ga_{0.7}N$ EBL shows heavy dependence on the p-doping level of EBL. As the doping concentration increases, the enhanced Φ_e holds back the transition of electrons to the

Table 3. Characteristics of $Al_{0.3}Ga_{0.7}N$ and $B_{0.14}Al_{0.86}N$ EBL structures with various doping concentrations at 90 mA.

LED structure	$Al_{0.3}Ga_{0.7}N$ EBL LED			$B_{0.14}Al_{0.86}N$ EBL LED		
Doping concentration	1×10^{18} cm^{-3}	1×10^{19} cm^{-3}	1×10^{20} cm^{-3}	1×10^{18} cm^{-3}	1×10^{19} cm^{-3}	1×10^{20} cm^{-3}
Thresholdvoltage	3.56 V	3.55 V	3.52 V	4.34 V	4.29 V	3.97 V
Resistance	39.5 Ω	39.4 Ω	39.1 Ω	48.2 Ω	47.7 Ω	44.1 Ω
WPE	11.6%	35.5%	58.6%	51.2%	52.2%	56.7%

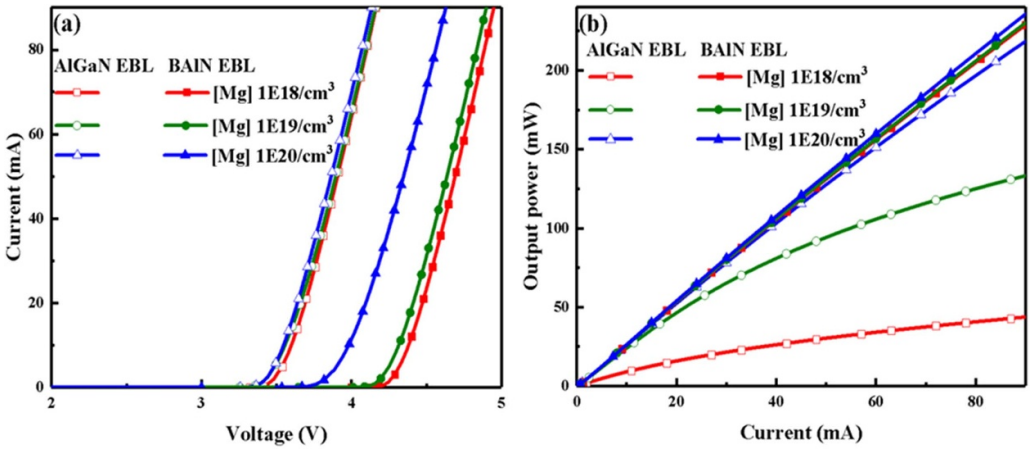

Figure 5. (a) *I*–*V* characterization curve of $Al_{0.3}Ga_{0.7}N$ and $B_{0.14}Al_{0.86}N$ EBL LEDs and (b) effect of p-doping level on output power for $Al_{0.3}Ga_{0.7}N$ and $B_{0.14}Al_{0.86}N$ EBL LEDs.

p-region. Meanwhile, the reduced Φ_h promotes the hole injection to the active region. By comparing IQE and output power features for the LEDs with an $Al_{0.3}Ga_{0.7}N$ EBL, we propose that the p-doping level of $Al_{0.3}Ga_{0.7}N$ EBL is preferable to be improved for high-performance UV LEDs. As for the LEDs with a $B_{0.14}Al_{0.86}N$ EBL, we show that the performance is less dependent on the p-doping level of EBL. With the decrease of doping concentration in $B_{0.14}Al_{0.86}N$ EBL, the Φ_e shows a downward trend but maintains at a high level and Φ_h shows an upward trend but maintains at a low level, respectively. Meanwhile, the electron and hole concentrations, IQE, as well as output power show less difference in different doping levels in the $B_{0.14}Al_{0.86}N$ EBL. We propose that the low-doping-level $B_{0.14}Al_{0.86}N$ EBL can still make a difference for acquiring high-performance UV LEDs.

4. Undoped EBL LED

It is well known that the generally adopted AlGaN EBL in UV LEDs will deteriorate the hole injection and introduce non-radiative recombination centers in MQWs [8]. Motivated by the diminutive valence band edge and large conduction band edge, we design the $B_{0.14}Al_{0.86}N$ EBL structures to avoid the p-doping issue. As discussed in part 3, the high p-doping level is not pre-requisite in designing EBL for LEDs after introducing the $B_{0.14}Al_{0.86}N$ EBL. To thoroughly demonstrate the potential of the undoped $B_{0.14}Al_{0.86}N$ EBL, we gather the effective barrier height of valence and conduction bands as a function of Mg doping concentration, as shown in figure 6. With low Mg doping concentration for both EBLs, the Φ_h and Φ_e barely decrease and increase with increasing doping concentration, respectively. Due to the relatively low activation energy of $B_{0.14}Al_{0.86}N$, the variations of Φ_e are more remarkable at the high p-doping level than that of $Al_{0.3}Ga_{0.7}N$. In contrast, the high-doping-level $B_{0.14}Al_{0.86}N$ EBL is expected to provide a larger Φ_e and a smaller Φ_h. It is noteworthy that when the doping concentration reduces to zero, the Φ_e of $B_{0.14}Al_{0.86}N$ EBL is 6.20 times that of $Al_{0.3}Ga_{0.7}N$ EBL, while the Φ_h of $B_{0.14}Al_{0.86}N$ EBL is 0.76 times that of $Al_{0.3}Ga_{0.7}N$ EBL. Thus, the low-doping-level $B_{0.14}Al_{0.86}N$ EBL still has great potential in reducing electron leakage and increasing hole injection, which is meaningful for the proposing of undoped $B_{0.14}Al_{0.86}N$ EBL.

To prove the superiority of undoped $B_{0.14}Al_{0.86}N$ EBL, we choose the undoped $B_{0.14}Al_{0.86}N$ EBL structure to compare with the $Al_{0.3}Ga_{0.7}N$ EBL structure with a high Mg doping concentration of 1×10^{20} cm^{-3}, which is deemed to be over the doping limit in the experiment [42]. As figure 7 illustrates, the undoped $B_{0.14}Al_{0.86}N$ EBL structure shows enhancements of the electron and hole concentrations in the QWs because it facilitates the blocking of electrons and hole transport into QWs simultaneously. Compared with the $Al_{0.3}Ga_{0.7}N$ EBL structure, the increased electron concentration in the QWs of the undoped $B_{0.14}Al_{0.86}N$ EBL structure is due to that the larger Φ_e can lead to a declined electron leakage. In the meantime, because the relatively low Φ_h promotes the

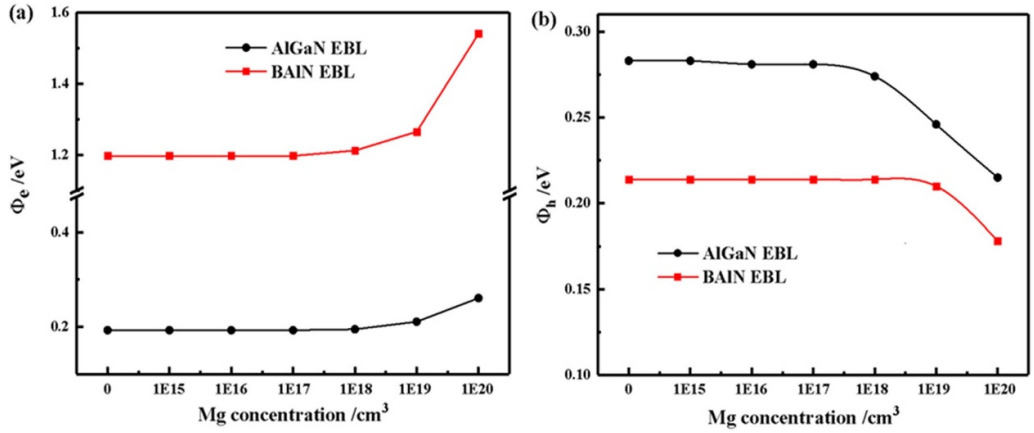

Figure 6. Effective barrier height of (a) conduction and (b) valence band for variously doped $Al_{0.3}Ga_{0.7}N$ and $B_{0.14}Al_{0.86}N$ EBL at 90 mA.

Table 4. Overlapping of wave functions of the undoped $B_{0.14}Al_{0.86}N$ EBL structure.

QWs	1st QW	2nd QW	3rd QW	4th QW	5th QW
Overlapping of wave functions	41.49%	41.35%	41.36%	41.38%	32.99%

hole injection, the hole concentration in QWs for undoped $B_{0.14}Al_{0.86}N$ EBL structure shows an enhancement compared with the $Al_{0.3}Ga_{0.7}N$ EBL structure. When it comes to the radiative recombination, an enhancement indicates that a higher intensity of emitting light can be achieved by the utilization of undoped $B_{0.14}Al_{0.86}N$ EBL. Besides, for the undoped $B_{0.14}Al_{0.86}N$ EBL structure, the electron and hole concentrations are the highest in the last QW, while the radiative recombination in the last QW is lowest. It can be attributed to the smallest overlapping of wave functions in the last QW, which is 32.99% as shown in table 4.

IQE is another vital parameter to evaluate the performance of the undoped LED. As shown in figure 8(a), the undoped $B_{0.14}Al_{0.86}N$ EBL structure displays a slightly increased peak efficiency of 74% and reduced efficiency droop ratio at 90 mA compared with that of $Al_{0.3}Ga_{0.7}N$ EBL structure. Figure 8(b) represents the output power, *I–V* curve, and WPE for both structures. A slight improvement of output power is achieved by employing undoped $B_{0.14}Al_{0.86}N$ EBL to replace $Al_{0.3}Ga_{0.7}N$ EBL. Both of the improved IQE and enhanced output power are ascribed to the subdued electron leakage and enhanced hole injection for the undoped $B_{0.14}Al_{0.86}N$ EBL structure. The threshold voltage of the undoped EBL is 4.38 V, while that value of AlGaN EBL is 3.52 V. The calculated WPE of the undoped $B_{0.14}Al_{0.86}N$ EBL structure is around 51%, which is slightly lower than the $Al_{0.3}Ga_{0.7}N$ EBL structure of 59%. The slightly low WPE is attributed to the large forward voltage induced by the higher band barrier height of the $B_{0.14}Al_{0.86}N$ EBL structure, and it will not lead to severe power dissipation.

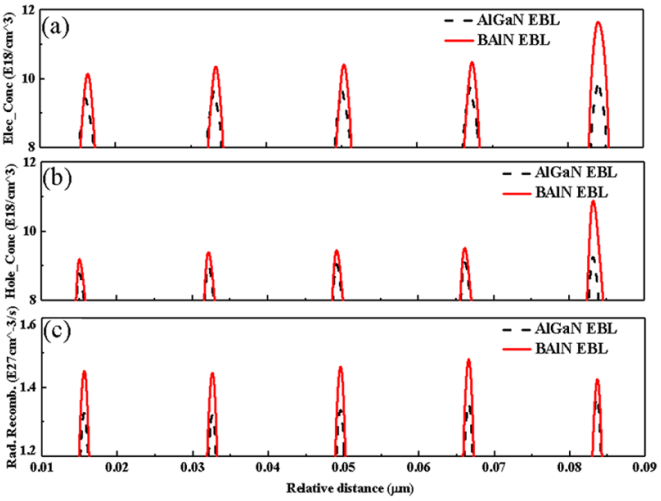

Figure 7. (a) Electron concentration, (b) hole concentration, and (c) radiative recombination rate in QWs for $Al_{0.3}Ga_{0.7}N$ EBL structures and undoped $B_{0.14}Al_{0.86}N$ EBL structures at 90 mA, respectively.

In summary, we propose an undoped $B_{0.14}Al_{0.86}N$ EBL structure to compare with the high-doping-level $Al_{0.3}Ga_{0.7}N$ EBL structure. The results show that the undoped $B_{0.14}Al_{0.86}N$ EBL structure still exhibits significant enhancements in blocking electrons and improving hole injection, because of the lager Φ_e and smaller Φ_h. As for the characterization curve, the $B_{0.14}Al_{0.86}N$ EBL structure shows comparable IQE and mitigates efficiency droop as well as elevated output power density compared with the $Al_{0.3}Ga_{0.7}N$ EBL structure. Moreover, the extremely challenging p-doping issue in the conventional AlGaN EBL can be alleviated by the employment of the undoped $B_{0.14}Al_{0.86}N$ EBL. Furthermore, the absence of doping for the EBL would avoid the quality deterioration by heavy Mg doping as in the AlGaN EBL. In addition, after the introducing of an undoped $B_{0.14}Al_{0.86}N$ EBL, the Mg diffusion issue, which is a well-known cause for lower radiative recombination rate, also can be relieved.

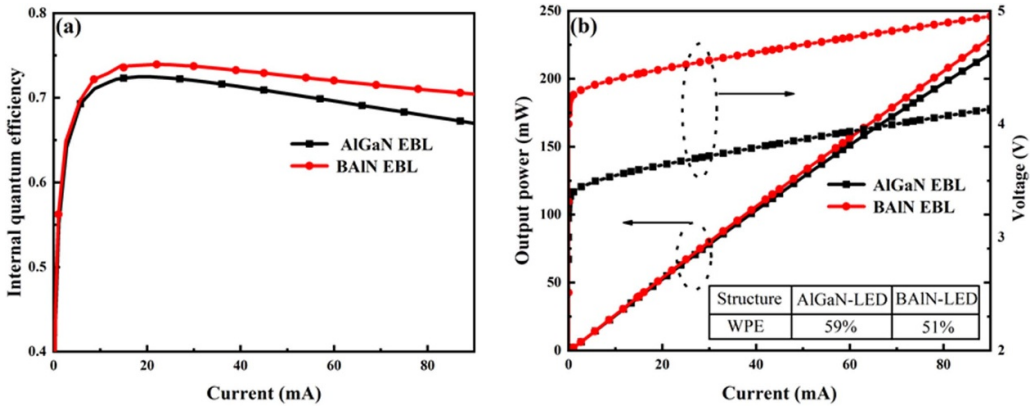

Figure 8. (a) IQE, and (b) output power features, *I*–*V* curve, and WPE for $Al_{0.3}Ga_{0.7}N$ and undoped $B_{0.14}Al_{0.86}N$ EBL LEDs.

5. Conclusion

The influence of various doping concentration $Al_{0.3}Ga_{0.7}N$ and $B_{0.14}Al_{0.86}N$ EBLs on the output features of UV LEDs has been systematically investigated. We reveal that the high doping level in $Al_{0.3}Ga_{0.7}N$ EBL is critical for the suppression of electron leakage and facilitates hole injection by elevated Φ_e and reduced Φ_h. As a result, for LEDs with an $Al_{0.3}Ga_{0.7}N$ EBL with a doping concentration of 1×10^{19} cm^{-3}, significant improvement in output power (208%) and enhanced IQE is achieved when compared with the LEDs with an $Al_{0.3}Ga_{0.7}N$ EBL at a doping concentration of 1×10^{18} cm^{-3}. When adopting a $B_{0.14}Al_{0.86}N$ EBL instead of the $Al_{0.3}Ga_{0.7}N$ EBL, the performance of UV LEDs shows less deterioration with the decrease of doping concentration due to the intrinsic large conduction band offset and pimping valence band offset at $B_{0.14}Al_{0.86}N/Al_{0.2}Ga_{0.8}N$ heterointerface. The comparison between the proposed undoped $B_{0.14}Al_{0.86}N$ EBL structure and the conventional highly doped $Al_{0.3}Ga_{0.7}N$ EBL structure further demonstrates the potential of $B_{0.14}Al_{0.86}N$ EBL in improving the performance of UV LEDs. Based on these results, we propose an undoped $B_{0.14}Al_{0.86}N$ EBL structure, which is compatible with doping-free and high performance. By the employment of undoped $B_{0.14}Al_{0.86}N$ EBL, the p-doping issue in the conventional $Al_{0.3}Ga_{0.7}N$ EBL can be alleviated and therefore the epitaxy progress can be simplified. This work offered a novel sight to design high-performance UV LEDs without considering the high p-doping issue.

Acknowledgments

The KAUST authors would like to acknowledge the support of KAUST Baseline Fund BAS/1/1664-01-01, GCC Research Council Grant REP/1/3189-01-01, and Competitive Research Grants URF/1/3437-01-01 and URF/1/3771-01-01. The authors of Institute of Semiconductors would like to acknowledge the support of National Key R&D Program of China 2016YFB0400800, National Natural Sciences Foundation of China 61875187, 61527814, 61674147, and U1505253, Beijing Nova Program Z181100006218007, and Youth Innovation Promotion Association CAS 2017157.

ORCID iDs

Wen Gu https://orcid.org/0000-0001-7248-3687
Rongyu Lin https://orcid.org/0000-0001-5780-2838
Zihui Zhang https://orcid.org/0000-0003-0638-1118
Jae-Hyun Ryou https://orcid.org/0000-0002-7397-6616
Xiaohang Li https://orcid.org/0000-0002-4434-365X

References

[1] Muramoto Y, Kimura M and Nouda S 2014 *Semicond. Sci. Technol.* **29** 084004
[2] Kneissl M *et al* 2010 *Semicond. Sci. Technol.* **26** 014036
[3] Hirayama H, Fujikawa S and Kamata N 2015 *Electr. Commun. Japan.* **98** 1
[4] Kneissl M, Seong T Y, Han J and Amano H 2019 *Nat. Photon.* **13** 233
[5] Kuo Y K, Chang J Y, Chen F M, Shih Y H and Chang H T 2016 Numerical Investigation on the Carrier Transport Characteristics of AlGaN Deep-UV Light-Emitting Diodes *IEEE J. Quantum Electron.* **52** 1
[6] He L, Zhao W, Zhang K, He C, Wu H, Liu N, Song W, Chen Z and Li S 2018 *Opt. Lett.* **43** 515
[7] Kuo Y K, Chen Y H, Chang J Y and Tsai M C 2012 *Appl. Phys. Lett.* **100** 043513
[8] Svensk O, Törmä P T, Suihkonen S, Ali M, Lipsanen H, Sopanen M, Odnoblyudov M A and Bougrov V E 2008 *J. Cryst. Growth* **310** 5154
[9] Jeon S R, Ren Z, Cui G, Su J, Gherasimova M, Han J, Cho H K and Zhou L 2005 *Appl. Phys. Lett.* **86** 082107
[10] Michałowski P P, Złotnik S, Sitek J, Rosiński K and Rudziński M 2018 *Phys. Chem. Chem. Phys.* **20** 13890
[11] Lin W Y, Wang T Y, Liang J H, Ou S L and Wuu D S 2014 *IEEE Trans. Electron Devices* **61** 3790
[12] Manfra M J, Pfeiffer L N, West K W, Stormer H L, Baldwin K W, Hsu J W, Lang D V and Molnar R J 2000 *Appl. Phys. Lett.* **77** 2888
[13] Kuo Y K, Chen F M, Lin B C, Chang J Y, Shih Y H and Kuo H C 2016 Simulation and experimental study on barrier thickness of superlattice electron blocking layer in near-ultraviolet light-emitting diodes *IEEE J. Quantum Electron.* **52** 8
[14] Kuo Y K, Yen S H and Chen J R 2006 Optoelectronic devices: physics, fabrication, and application III *Int. Society for Optics and Photonics* **6368** 636812
[15] Ren Z *et al* 2019 *IEEE Photon. J.* **11** 820051
[16] Le-Juan W *et al* 2012 *Chin. Phys.* B **21** 068506

[17] Zhang Y *et al* 2015 *Superlattices Microstruct.* **82** 151
[18] Fan X, Sun H, Li X, Sun H, Zhang C, Zhang Z and Guo Z 2015 *Superlattices Microstruct.* **88** 467
[19] Satter M M, Liu Y S, Kao T T, Lochner Z, Li X, Ryou J H, Shen S C, Detchprohm T, Dupuis R D and Yoder P D 2014 *Phys. Status Solidi* c **11** 828
[20] Satter M M, Lochner Z, Kao T T, Liu Y S, Li X H, Shen S C, Dupuis R D and Yoder P D 2014 *IEEE J. Quantum Electron.* **50** 166
[21] Hu W, Qin P, Song W, Zhang C, Wang R, Zhao L, Xia C, Yuan S, Yin Y and Li S 2016 *Superlattices Microstruct.* **97** 353
[22] Abid M *et al* 2012 *Appl. Phys. Lett.* **100** 051101
[23] Sun H *et al* 2017 *Appl. Phys. Express* **11** 011001
[24] Li X, Wang S, Liu H, Ponce F A, Detchprohm T and Dupuis R D 2017 *Phys. Status Solidi* b **254** 1600699
[25] Liu K, Sun H, AlQatari F, Guo W, Liu X, Li J, Torres Castanedo C G and Li X 2017 *Appl. Phys. Lett.* **111** 222106
[26] Sun H, Park Y J, Li K H, Liu X, Detchprohm T, Zhang X, Dupuis R D and Li X 2018 *Appl. Surf. Sci.* **458** 949
[27] Sun H, Park Y J, Li K H, Torres Castanedo C G, Alowayed A, Detchprohm T, Dupuis R D and Li X 2017 *Appl. Phys. Lett.* **111** 122106
[28] APSYS (Burnaby, BC: Crosslight Software Inc.) (https://crosslight.com/products/apsys/) (available at: www.crosslight.com)
[29] Verzellesi G, Saguatti D, Meneghini M, Bertazzi F, Goano M, Meneghesso G and Zanoni E 2013 *J. Appl. Phys.* **114** 10
[30] Liu K, AlQatari F, Sun H, Li J, Guo W and Li X 2018 (arXiv:1808.07211)
[31] Dreyer C E, Janotti A, van de Walle C G and Vanderbilt D 2016 *Phys. Rev.* X **6** 021038
[32] Zhang M and Li X 2017 *Phys. Status Solidi* b **254** 1600749
[33] Coughlan C, Schulz S, Caro M A and O'Reilly E P 2015 *Phys. Status Solidi* b **252** 879
[34] Piprek J, Römer F and Witzigmann B 2015 *Appl. Phys. Lett.* **106** 101101
[35] Yun J, Shim J and Hirayama H 2015 *Appl. Phys. Lett.* **8** 022104
[36] Zhang Z, Zhang Y, Bi W, Geng C, Xu S, Demir H and Sun X 2016 *Appl. Phys. Lett.* **109** 239901
[37] Lu T, Li S, Zhang K, Liu C, Yin Y, Wu L, Wang H, Yang X, Xiao G and Zhou Y 2011 *Opt. Express* **19** 18319
[38] Fiorentini V, Bernardini F and Ambacher O 2002 *Appl. Phys. Lett.* **80** 1204
[39] Götz W, Johnson N M, Walker J, Bour D P and Street R A 1996 *Appl. Phys. Lett.* **68** 667
[40] Nam K B, Nakarmi M L, Li J, Lin J Y and Jiang H X 2003 *Appl. Phys. Lett.* **83** 878
[41] Vurgaftman I and Meyer J N 2003 *J. Appl. Phys.* **94** 3675
[42] Takano T, Mino T, Sakai J, Noguchi N, Tsubaki K and Hirayama H 2017 *Appl. Phys. Express* **10** 031002